Longitudinal Strength of Ships in Rough Seas

by Yoshiyuki Yamamoto, Masataka Fujino** and Toichi Fukasawa****

In this paper, the longitudinal strength of ships in rough seas are investigated taking account of slamming. Illustrative calculations are performed for two ships; a fast container ship with large bow-flare and a full-bodied large bulk carrier in fully laden condition. In the former case, the longitudinal vertical bending moment in the main hull girder is investigated in case of bow-flare slamming, and the interactions of bottom and bow-flare slamming are clarified. Besides the calculations, a series of tank tests is conducted in a basin to confirm the theory, making use of an elastic model ship. In the latter case, special interests are concentrated to the occurrence of serious bottom slamming for full-bodied ships in the fully laden conditions.

1. Introduction

In order to investigate the longitudinal strength of a ship due to slamming, the following procedure called "two-steps analysis" has so far been employed; first, the ship's motions in waves are calculated by a linear theory, such as the strip method, and then longitudinal vertical bending moments are calculated using the equivalent external forces including slamming impacts derived from the ship's motions.[1-5] The linear strip theory has been a powerful tool for predicting a ship's motions among infinitesimal waves. In rough seas, however, nonlinear effects like slamming impacts become significant, and responses of a ship differ from those estimated by the linear theory. In case of slamming, therefore, the hydro-elastic interactions cannot be ignored.[6-8]

Recently, increasing attentions have been paid to the measurements of bending moments of a ship in waves in relation to the longitudinal strength and springing[9-10], making use of the so-called segmented model connected rather rigidly. The model, however, cannot be used for the investigations of rapid responses to localized slamming impacts, because they cause whipping vibrations. Experiments should be done with the use of elastic models for this purpose, to obtain the time histories of elastic strains. The laws of similitude for elasticity should be satisfied in this case, beside the Froude scaling law.[11]

In the present paper, the motion and longitudinal strength of ships among waves of high wave height are investigated on the basis of a concept similar to the strip theory, taking account of such nonlinearities as the hull configurations of the ship, bottom emergence, and bottom and/or bow-flare slamming. Illustrative calculations were performed for two ships; a fast container ship with large bow-flare in regular waves, and a full-bodied large bulk carrier in fully laden condition in irregular waves. A series of tank tests were carried out to confirm the validity of the theory making use of an elastic model of the container ship.

2. Formulation

The rectangular coordinate system (X, Y, Z) is introduced so that the X, Y-plane lies on the still water surface and the Z-axis directs downward as shown in Fig. 1. Let a ship travel with constant speed U in the direction of the angle χ with the X-axis, and introduce

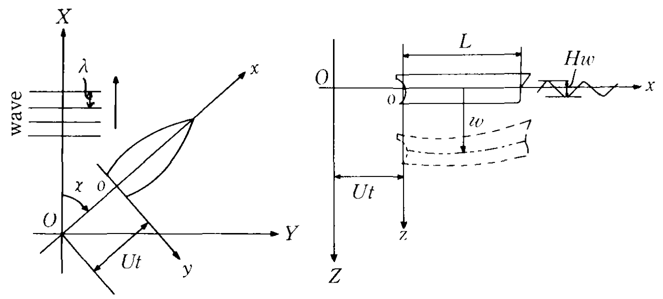

Fig.1 Coordinate system

the coordinate system (x, y, z) moving with the ship so that the x, y-plane lies in the X, Y-plane and the z-axis directs downward. Consider a wave train travelling in the direction of positive X.

Regarding the ship's hull as an elastic beam, the equation of vertical motion of the ship's hull can be described in terms of the displacement component w in the z-direction; that is

$$\mu\frac{\partial^2 w}{\partial t^2}+\frac{\partial^2}{\partial x^2}\left[EI_z\frac{\partial^2 w}{\partial x^2}+\eta EI_z\frac{\partial^3 w}{\partial t\partial x^2}\right]=f_e \quad \cdots\cdots(1)$$

where μ, EI_z, η, and f_e are the mass per unit length, the flexural rigidity for vertical bending, the structural damping coefficient, and the external force, defined at a section of the ship.

On the basis of the concept of the strip theory, the

* Department of Naval Architecture, University of Tokyo; Chairman of Subcommittee, Technical Committee of the Society
** Department of Naval Architecture, University of Tokyo *** Institute of Engineering Mechanics, University of Tsukuba

external force caused by the momentum changes of fluid is given by

$$f_m = -\frac{D}{Dt}\left[M_H\left\{\frac{D}{Dt}(w+y_m\phi)-v_z\right\}\right] \cdots\cdots (2)$$

where M_H, y_m, ϕ, and v_z are the time-varying sectional added mass for vertical motion, the y-coordinate of the acting point of pressure related to M_H, the rotating angle of a section, and the vertical component of the orbital velocity of the incident waves, and

$$\frac{D}{Dt}=\frac{\partial}{\partial t}-U\frac{\partial}{\partial x} \cdots\cdots (3)$$

The damping force f_r due to wave-making is in proportion to the relative velocity as described as follows;

$$f_r = -N_H\left\{\frac{D}{Dt}(w+y_r\phi)-v_z\right\} \cdots\cdots (4)$$

where N_H and y_r are the time-varying sectional damping coefficient due to wave-making for vertical motion and the y-coordinate of the acting point of pressure related to N_H.

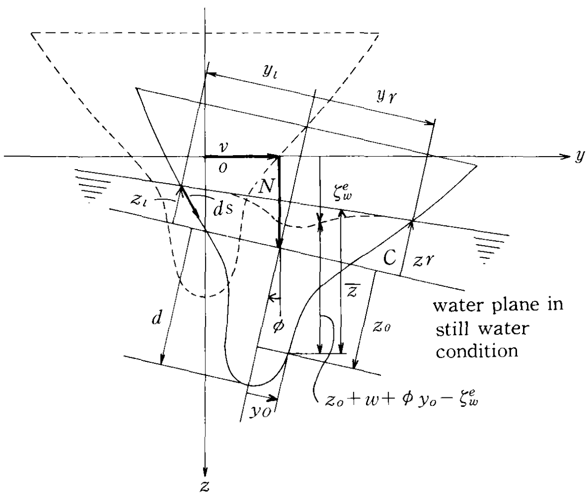

Fig.2 Ship section and wave surface

The pressure force f_p is obtained by integrating the pressure, p, over the wetted surface, C, of the hull; that is

$$f_p=\int_C (-p)\, n_z ds \cdots\cdots (5)$$

where n_z is the z-component of the outward unit-vector normal to the ship's hull in a section. Introducing the velocity potential Φ for the incident waves, the pressure is derived from Bernoulli's equation; that is

$$p=-\rho\frac{D\Phi}{Dt}+\rho g(z_0+w+y_0\phi) \cdots\cdots (6)$$

where ρ, g, y_0 and z_0 are the mass density of water, the acceleration due to gravity, y-, and z-coordinate of a point on the hull in still water, respectively (see Fig. 2). Introducing Eq.(6) into Eq.(5) leads to

$$f_p=\rho g A \cdots\cdots (7)$$

where

$$A=\int_{y_l}^{y_r}(z_0+w+y_0\phi-\zeta_w^e)\,dy_0 \cdots\cdots (8)$$

The effective wave elevation ζ_w^e is defined as

$$\zeta_w^e=\frac{1}{g}\frac{D\Phi}{Dt} \cdots\cdots (9)$$

which is the function of x, y_0 and z_0.

Since the weight per unit length is given by

$$f_g=\mu g \cdots\cdots (10)$$

the total external force becomes as

$$f_e=f_m+f_r+f_p+f_g \cdots\cdots (11)$$

The numerical procedure for solving Eq.(1) is based on the Galerkin method: Assume that the displacement w is represented in a linear combination of four normal functions for a uniform free-free beam; that is

$$w=\sum_{j=0}^{3}W_j(x)\,q_j(t) \cdots\cdots (12)$$

where $W_j(x)$ is a normal function of the j-th mode given by

$$W_0=1.0$$
$$W_1=\frac{x}{L}-0.5 \cdots\cdots (13)$$
$$W_j=\cos\lambda_j x+\cosh\lambda_j x-c_j(\sin\lambda_j x+\sinh\lambda_j x)$$
$$(j=2,3)$$

where

$$c_j=(\cos\lambda_j L-\cosh\lambda_j L)/(\sin\lambda_j L-\sinh\lambda_j L)$$
$$\lambda_2 L=4.73 \text{ and } \lambda_3 L=7.8532 \cdots\cdots (14)$$

The generalized coordinate $q_j(t)$ is determined by the following matrix equation, which is obtained by introducing Eq.(12) into Eq.(1) and applying the Galerkin method to the resulting equation:

$$[M_{ij}]\{\ddot{q}_i\}+[C_{ij}]\{\dot{q}_i\}+[K_{ij}]\{q_i\}=\{f_i\} \cdots (15)$$

where

$$M_{ij}=\int(\mu+M_{Hj})\,W_iW_jdx$$

$$C_{ij}=\int\eta_j EI_z W_i'' W_j'' dx+\int N_{Hj}W_iW_jdx+\int M_{Hj}W_iW_jdx$$
$$-U\int M_{Hj}W_iW_j'dx+U\int M_{Hj}W_i'W_jdx-U\left[M_{Hj}W_iW_j\right]_0^L$$

$$
\begin{aligned}
K_{ij}&=\int EI_z W_i'' W_j'' dx - U\int N_{Hj} W_i W_j' dx \\
&- U\int \dot{M}_{Hj} W_i W_j' dx \\
&- U^2\int M_{Hj} W_i' W_j' dx + U^2[M_{Hj} W_i W_j']_0^L \\
f_i&=\int M_{He}\dot{v}_z W_i dx + \int N_{He} v_z W_i dx \\
&+ \int \dot{M}_{He} v_z W_i dx \\
&+ U\int M_{He} v_z W_i' dx + \rho g\int \mu W_i dx - g\int A W_i dx \\
&- U[M_{He} v_z W_i]_0^L \quad \cdots\cdots\cdots (16)
\end{aligned}
$$

Although they are frequency-dependent, the added mass and the damping coefficients, M_H and N_H, can be assumed to take certain constant values for each mode. The values of M_{Hj} and N_{Hj} should be appropriately chosen according to the mode; they are determined by the encounter frequency for rigid-body modes ($j=0, 1$), and are assumed to be frequency-independent for vibration modes ($j=2, 3$). The subscript e means the quantity defined for the encounter frequency. The structural damping coefficient η_j is determined by modifying the logarithmic decrement δ observed on type-ships in still water[12]; that is

$$
\begin{cases} \eta_j=0 & \text{for rigid-body modes} \\ \eta_j=\delta/\pi\omega_{2v} & \text{for vibration modes} \end{cases} \quad \cdots (17)
$$

where ω_{2v} is the natural frequency for 2-node vertical vibration in water.

As for the rotating angle ϕ, it will be assumed that the ship rotates as rigid-body; the torsion of a ship is neglected and the rolling motion is only taken into account. Hereafter, the rolling motion will be calculated by means of the linear strip theory.

In the following, Eq. (15) will be integrated with the aid of a Newmark-β method with $\beta=1/4$, taking account of the nonlinear effects. The method is adopted from the viewpoint of stability and accuracy of the numerical solutions.

The numerical procedure for nonlinearities are as follows:

Impact Force The most significant term in the expression given by Eq. (2) is the impact force; that is

$$
f_{\rm imp}=-\frac{\partial M_H}{\partial t}\left\{\frac{D}{Dt}(w+y_m\phi)-v_z\right\} \quad \cdots\cdots\cdots (18)
$$

which is in proportion to the square of the relative velocity of the ship to the water[7]. It will be assumed that the impact force will be disregarded when the ship's section is departing from water; namely

$$
\begin{cases} f_{\rm imp}=-\dfrac{\partial M_H}{\partial t}\left\{\dfrac{D}{Dt}(w+y_m\phi)-v_z\right\}, & \text{if } V_{\rm rel}>0 \\ f_{\rm imp}=0, & \text{if } V_{\rm rel}<0 \end{cases}
$$

$$
\cdots\cdots\cdots\cdots\cdots\cdots\cdots\cdots\cdots\cdots\cdots\cdots (19)
$$

where

$$
V_{\rm rel}=\frac{D}{Dt}(w+y_m\phi)-v_z \quad \cdots\cdots\cdots\cdots\cdots\cdots (20)
$$

This assumption was confirmed by the experiment of which the results is shown in Fig. 3. The time derivative

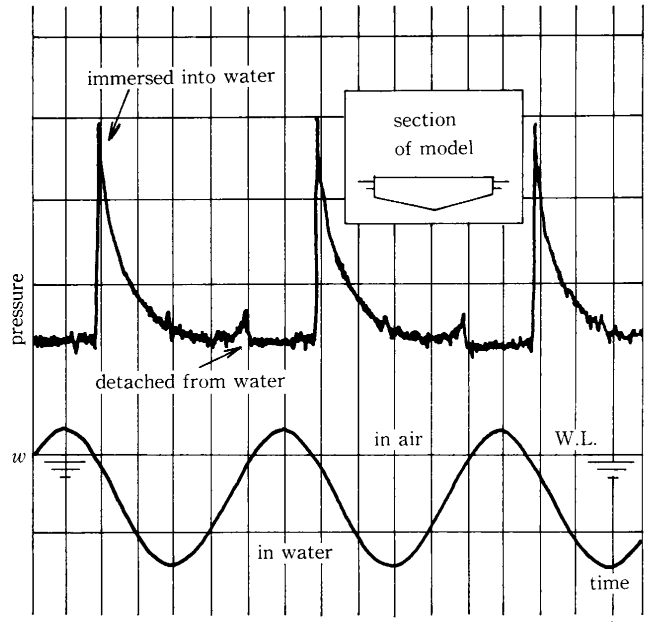

Fig.3 Time history of impact pressure

of the added mass included in Eq. (19) is evaluated as follows;

$$
\begin{cases} \dfrac{\partial M_H}{\partial t}=\dfrac{M_H|\bar{z}=0}{\Delta t}, & \text{for bottom impact} \\ \dfrac{\partial M_H}{\partial t}=\dfrac{\partial M_H}{\partial \bar{z}}\dfrac{\partial \bar{z}}{\partial t}, & \text{otherwise} \end{cases} \quad (21)
$$

where Δt is a discrete time interval used for time integration.

Bottom Emergence For a ship section apart from water, the external forces except the weight are not taken into account.

Hull Shape Nonlinearity The added mass, the damping coefficient due to wave-making, and the pressure force are calculated according as the instantaneous draft.

3. Fast Container Ship with Large Bow-Flare

3.1 Vertical Bending Moment on an Actual Ship

The body plan of the container ship used for the following analysis is shown in Fig. 4, which is characterized by large bow-flare. The principal dimensions of the ship are as follows;

$$
L\times B\times D=175.0\,\text{m}\times 25.2\,\text{m}\times 15.3\,\text{m}
$$
$$
d_{\rm aft}=9.940\,\text{m},\ d_{\rm fore}=9.507\,\text{m}
$$

The ship is in fully laden condition and the weight distribution is assumed to be equal to that of buoyancy. Structural data used are as follows[13];

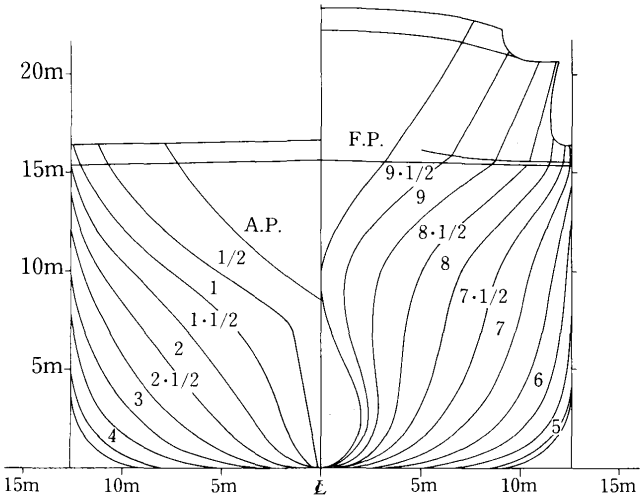

Fig.4 Body plan of container ship

$\delta = 0.056$
$I_z = 92.0\ \mathrm{m}^4$ at midship

The regular wave trains are considered as the incident wave. The ship in regular wave is subjected to slamming successively, and it is noted here that unrealistically large structural damping is assumed until the oscillatory motions fully develop in order to eliminate whipping vibrations due to the previous slamming.

Effects of the reduction of the ship's speed and the heading angle will be investigated in the following. It is also assumed that the rolling motion of the ship is disregarded; it is valid as far as changing of the heading angle is small.

Effects of Reduction of Ship Speed Time histories of vertical bending moment are shown in Figs. 5−7, for various ship's speeds. It can be seen that the responses depend largely upon the ship's speed. The hydrodynamic impact may occur at bottom and bow-flare successively in this case. The time interval τ between bottom and bow-flare impacts becomes important for elastic

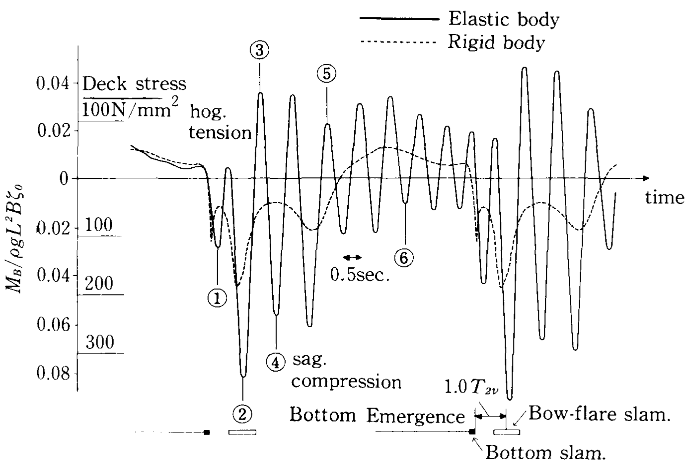

Fig.5 Time history of vertical bending moment at midship
($Fn = 0.261$, $\chi = 180°$, $\lambda/L = 1.2$, $L/Hw = 14.5$)

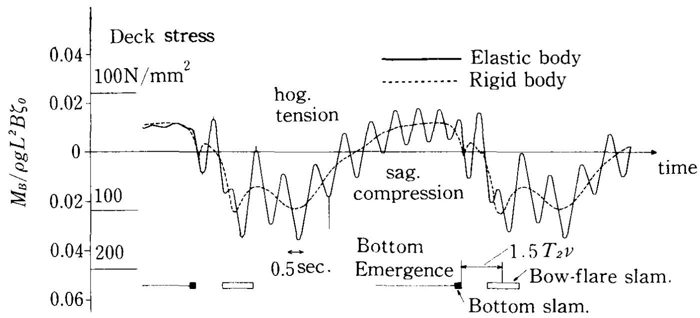

Fig.6 Time history of vertical bending moment at midship
($Fn = 0.15$, $\chi = 180°$, $\lambda/L = 1.2$, $L/Hw = 14.5$)

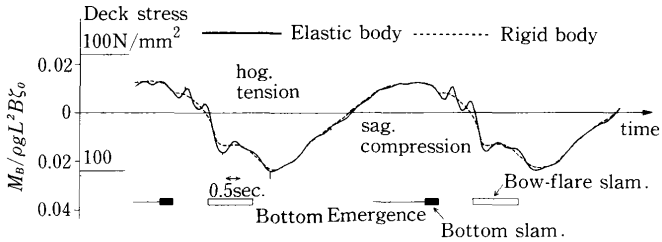

Fig.7 Time history of vertical bending moment at midship
($Fn = 0.07$, $\chi = 180°$, $\lambda/L = 1.2$, $L/Hw = 14.5$)

responses of the ship, therefore. In case of high speed (Fig. 5), the time interval τ is roughly equal to 1.0 T_{2v}, where T_{2v} is the ship's average natural period of the 2 node vibration; effects of bow-flare impacts are superposed on those of bottom impacts. On the other hand, vibrations caused by bottom and bow-flare impacts are canceled out when $\tau = 1.5\ T_{2v}$, as shown in Fig.6 (medium speed). In Fig.7 (low speed), the impact force decreases significantly, because of low relative velocity between the ship and wave surface. For preventing serious structural damages due to whipping vibrations, therefore, reduction of the ship's speed is recommended as an effective means in handling of container ships. Longitudinal distribution of the vertical

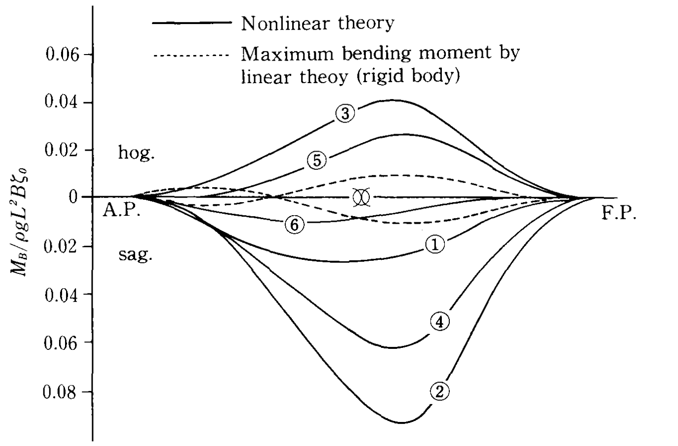

Fig.8 Longitudinal distribution of vertical bending moment
($Fn = 0.261$, $\chi = 180°$, $\lambda/L = 1.2$, $L/Hw = 14.5$)

bending moment is shown in Fig.8 (high speed), in which large bending moments occur at the rather fore-body.

Effects of Small Changing of Heading Angle

In the case when waves are in the 22.5° port or starboard direction, the calculations show almost the same results as in the right head sea (compare Figs. 9 and 10 with Figs. 5 and 8). If the ship has large angle against waves, the whipping vibrations decrease; however, the other problems may occur as the rolling motions, the difficulty for keeping her courses, and so on.

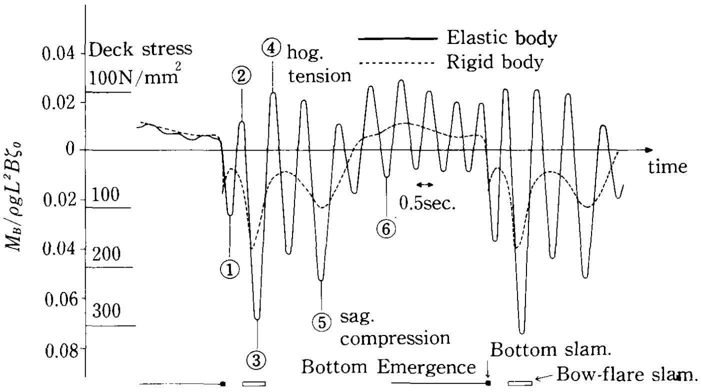

Fig.9 Time history of vertical bending moment at midship ($Fn=0.261$, $\chi=157.5°$, $\lambda/L=1.2$, $L/Hw=14.5$)

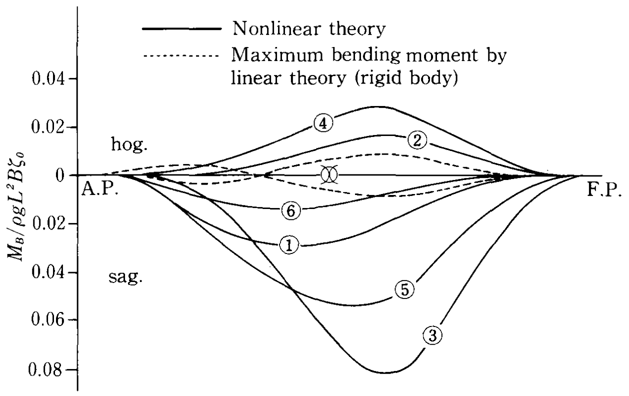

Fig.10 Longitudinal distribution of vertical bending moment

($Fn=0.261$, $\chi=157.5°$, $\lambda/L=1.2$, $L/Hw=14.5$)

3.2 Experiments with an Elastic Model Ship

In order to simulate the whipping vibrations of ships by experiments, the model ship should be made to satisfy the laws of similitude for elasticity. For designing an elastic model ship of linear scale α, the following relations should be satisfied according to the laws of similitude[11,14];

$$L_m=\alpha L_s \quad \cdots\cdots (22)$$

$$(EI)_m=\alpha^5 (EI)_s \quad \cdots\cdots (23)$$

$$U_m=\sqrt{\alpha}\, U_s \quad \cdots\cdots (24)$$

$$\lambda_m=\alpha \lambda_s \quad \cdots\cdots (25)$$

$$(H_w)_m=\alpha (H_w)_s \quad \cdots\cdots (26)$$

$$T_m=\sqrt{\alpha}\, T_s \quad \cdots\cdots (27)$$

where T is a characteristic time duration related to external loads, and the subscripts s and m indicate the full-scale or model ship, respectively. Eq.(23) is the restrictions required at designing the model, Eqs. (24) to (26) are the conditions required at executing the tests, and Eq.(27) directly follows from the others if loads are governed only by the ship-wave interactions.

It is difficult to satisfy Eq.(23) with the use of metallic materials in general, particularly in the case of small α. In the present investigation, foamed vinyl chloride is chosen as the structural material of the elastic model to satisfy Eq. (23). The particulars of the model are shown

Table 1 Particulars of model

Length between Perpendiculars	(L)	3.0000m
Breadth Moulded	(B)	0.4320m
Depth Moulded	(D)	0.2620m
Draft at A.P.	(d_a)	0.1704m
Draft at Midship	(d_m)	0.1667m
Draft at F.P.	(d_f)	0.1630m
Displacement	(Δ)	124.6000kg
Block Coefficient	(C_b)	0.5787
Center of Gravity from Midship	(x_G)	1.54% L fore
Radius of Gyration for Pitching	(κ_l)	0.2380L
GM		0.0354B

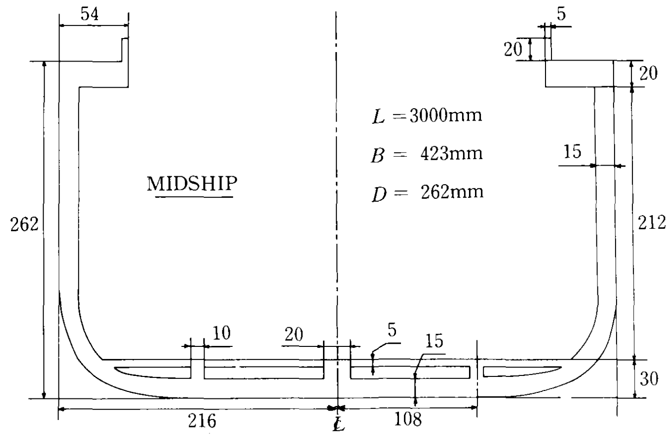

Fig.11 Scantling of midship section of model

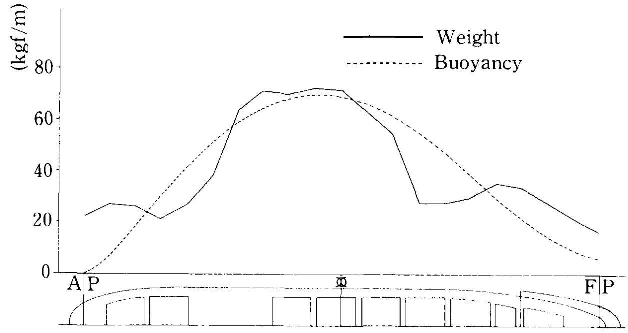

Fig.12 Weight and buoyancy distributions of model

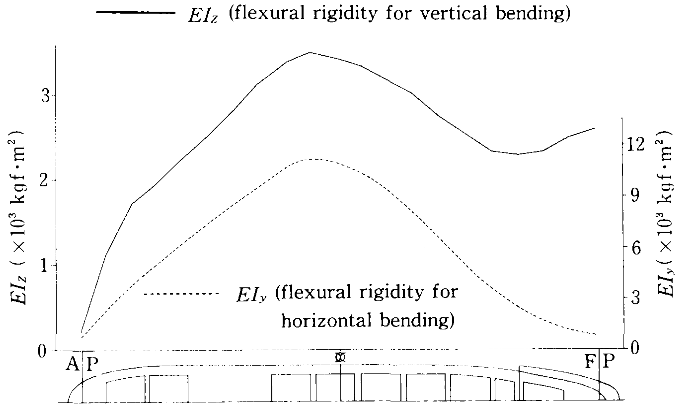

Fig.13 Distribution of flexural rigidity of model

in Table 1 and the scantling of the midship section in Fig. 11, which is a 1/58.33 model of the container ship mentioned before. The model tests were carried out for fully laden condition with the self-propulsive model. The weight and buoyancy, and the flexural rigidity diagrams are shown in Figs. 12 and 13. The logarithmic decrement of the model is measured as

$$\delta = 0.284$$

in still water. This large damping characteristics make it possible to damp the vibrations caused by previous slams rapidly, and the whipping vibrations caused by respective slams can easily be recognized.

A series of tank tests were conducted in the Seakeeping and Maneuvering Basin in the University of Tokyo. The following data were recorded; wave elevations, angles of pitch, roll, and yaw, vertical bow acceleration, pressure at bow-flare, and deck strains in the longitudinal direction. The locations of the gauges are shown in Fig. 14. The tests were carried out in

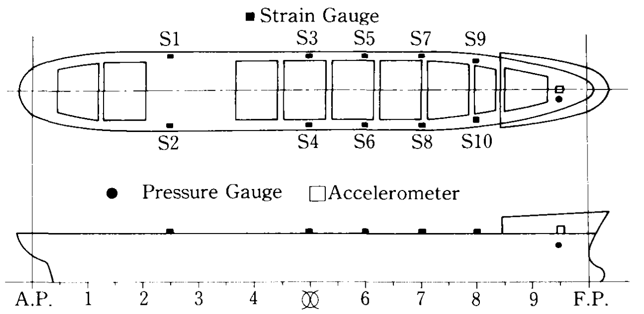

Fig.14 Locations of gauges

regular waves of various conditions: Encounter angle χ, length λ, and height H_w of waves were as follows;

$$\chi = 180°,\ 157.5°,\ 135°,\ 90°,\ 45°,\ 0°$$
$$\lambda/L = 0.8,\ 1.0,\ 1.2,\ 1.5$$
$$L/H_w = 30,\ 20,\ 15$$

The number of the propeller revolutions were adjusted so that the Froude number was 0.15, 0.24, or 0.33 in still water; in reality, significant speed losses were observed in waves (see Fig. 15).

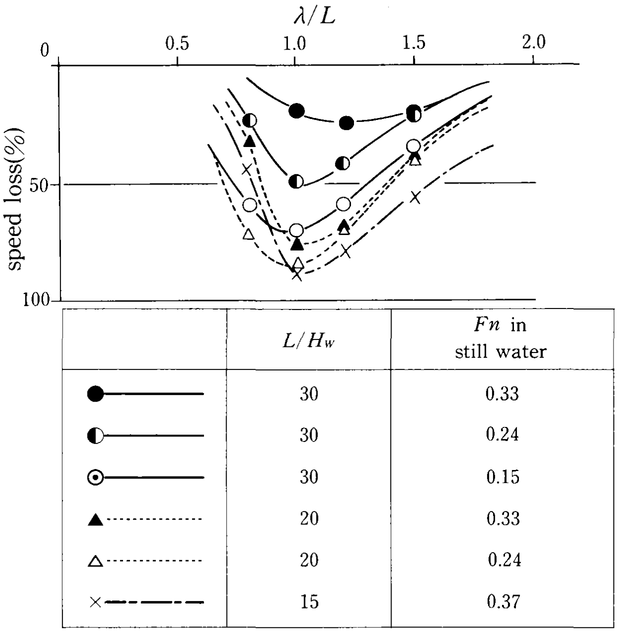

Fig.15 Speed loss in head sea

Since the interests of this paper is the longitudinal strength of ships in slamming, the results are confined to the characteristics of deck-strains only when slamming may occur.

Head Sea Theoretical and experimental time histories of deck-strains are shown in Figs. 16 and 17

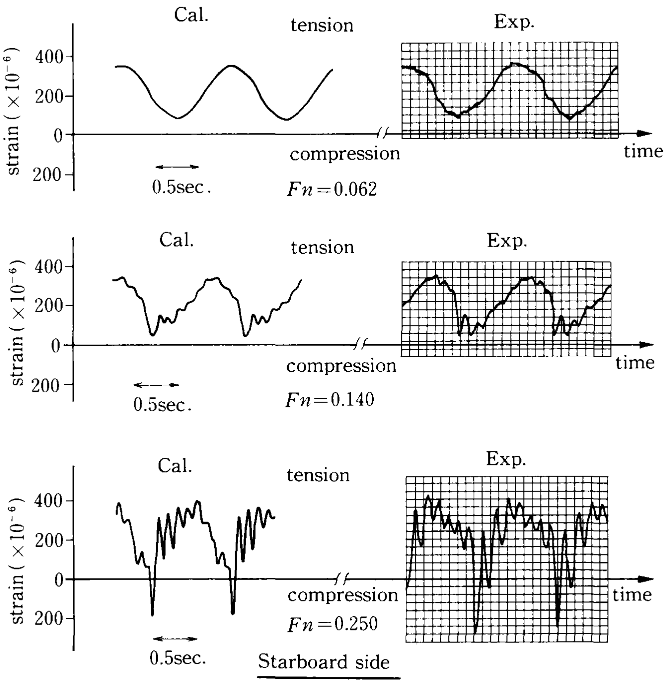

Fig.16 Time history of deck strain at midship
($\chi=180°$, $\lambda/L=1.2$, $L/Hw=30$)

for three kinds of the ship's speed. With the increase of the ship's speed, slams become heavier, which are observed in both experiments and calculations. The absolute values of deck-strain amplitudes obtained by the calculations show good agreement with experiments.

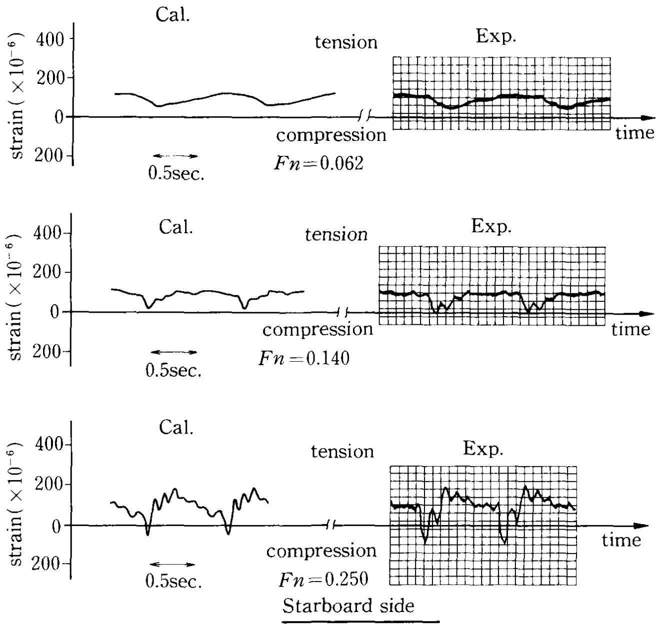

Fig.17 Time history of deck strain at S.S.8
(χ=180°, λ/L=1.2, L/Hw=30)

The difference between calculations and experiments at Fn = 0.250, as shown in Fig. 16, is related to the phase lag between bottom and bow-flare impacts; the dynamic swell-up of water is disregarded in the calculations.

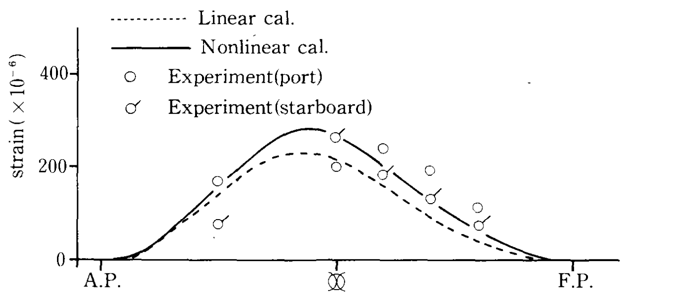

Fig.18 Longitudinal distribution of deck strain amplitudes
(Fn=0.062, χ=180°, λ/L=1.2, L/Hw=30)

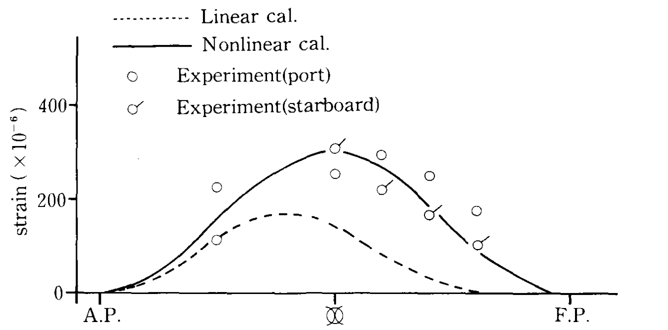

Fig.19 Longitudinal distribution of deck strain amplitudes
(Fn=0.140, χ=180°, λ/L=1.2, L/Hw=30)

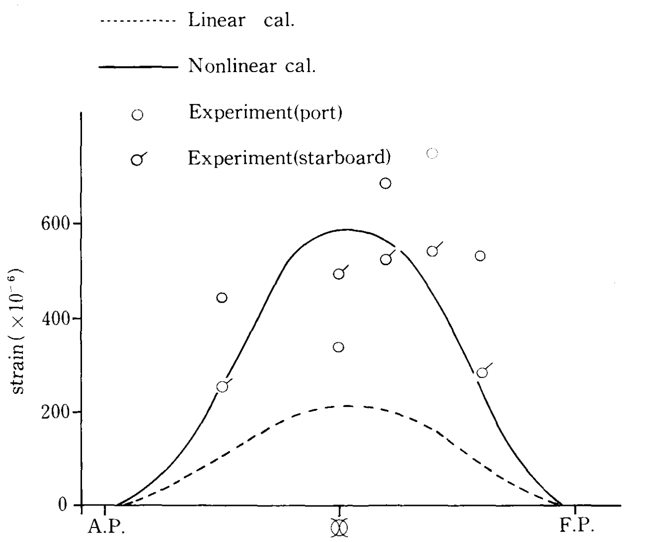

Fig.20 Longitudinal distribution of deck strain amplitudes
(Fn=250, χ=180°, λ/L=1.2, L/Hw=30)

In Figs. 18 to 20, longitudinal distributions of peak-to-peak values of deck-strains are shown. At high speed (Fn =0.140, 0.250), strains in the fore-body are more than twice those obtained by the linear theory, but they are in conformity with the nonlinear theory. On the other hand, both linear and nonlinear theories show good agreements with experiments at low speed (Fn=0.062).

Oblique Waves Slamming was observed only in bow waves (χ=157.5°,135°), and the angle of the rolling motions were very small in this case. This concludes that the effects of rolling motions can be disregarded when the longitudinal strength of ships due to slamming are considered.

The deck-strains in the longitudinal direction are, of course, caused by the vertical bending and horizontal bending in oblique waves. The horizontal bending moments are calculated by the linear strip theory in this paper, and the calculated time histories of deck-strains

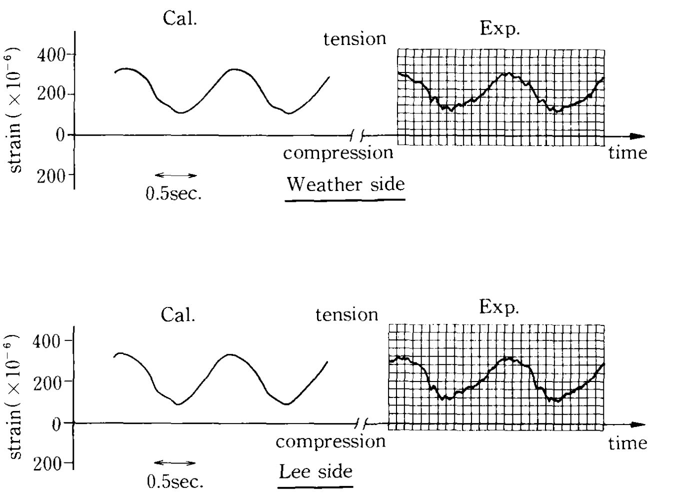

Fig.21 Time history of deck strain at midship
(Fn=0.067, χ=157.5°, λ/L=1.2, L/Hw=30)

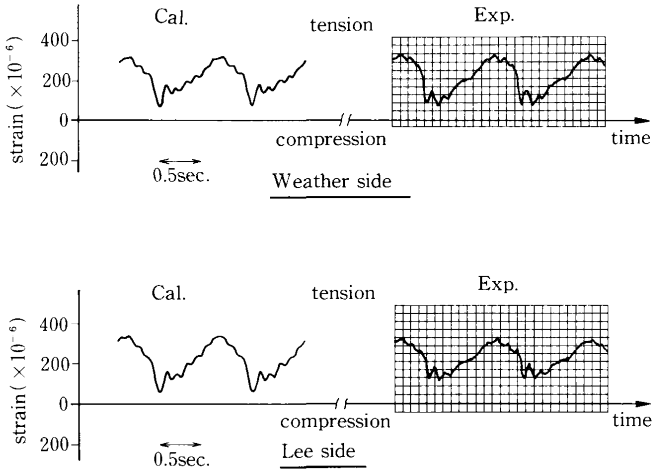

Fig.22 Time history of deck strain at midship
($Fn=0.152$, $\chi=157.5°$, $\lambda/L=1.2$, $L/Hw=30$)

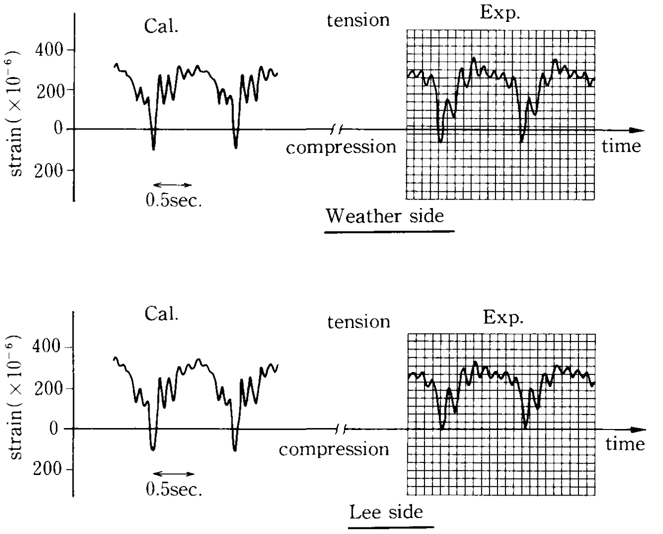

Fig.23 Time history of deck strain at midship
($Fn=0.232$, $\bar{\chi}=157.5°$, $\lambda/L=1.2$, $L/Hw=30$)

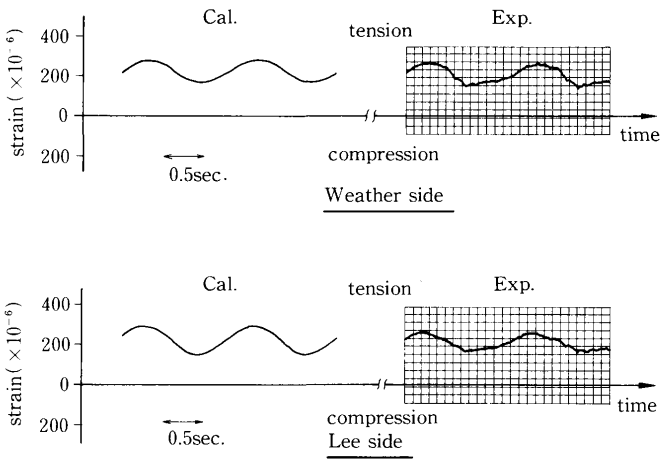

Fig.24 Time history of deck strain at midship
($Fn=0.081$, $\chi=135°$, $\lambda/L=1.2$, $L/Hw=30$)

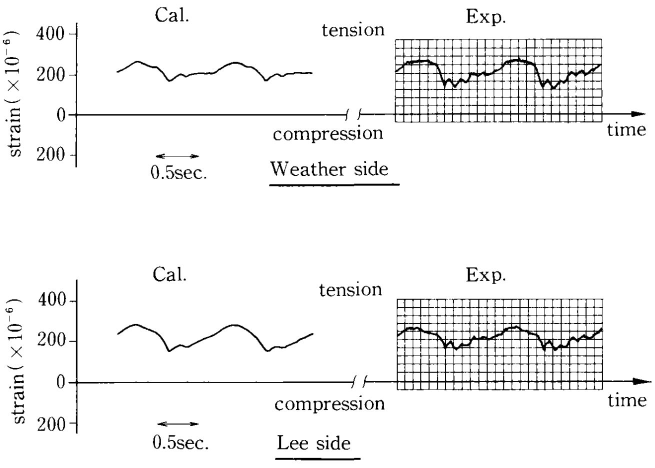

Fig.25 Time history of deck strain at midship
($Fn=0.164$, $\chi=135°$, $\lambda/L=1.2$, $L/Hw=30$)

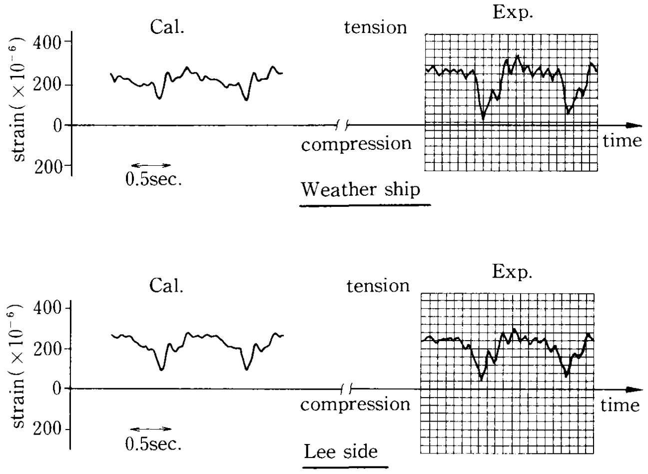

Fig.26 Time history of deck strain at midship
($Fn=0.262$, $\chi=135°$, $\lambda/L=1.2$, $L/Hw=30$)

are shown in Figs. 21 to 26 with the results of experiments. The general characteristics of deck-strains are the same as those in head sea, and it can be seen that the dack-strains in bow waves are slightly influenced by the horizontal bending moment in case of slamming.

4. Full-Bodied Large Bulk Carrier in Fully Laden Condition

It has been accepted so far that the serious bottom slamming does not occur on ships in fully laden conditions. It is revealed, however, that serious bottom slamming may occur by chance in full-bodied ships even in the fully laden condition.[15,16] The occurrence of the serious bottom slamming necessitates the following conditions;

a) bottom emergence due to rather high wave crest,
b) high relative velocity of the ship to the wave surface, and
c) small inclination between the bottom and the wave surface at the instant of bottom impact.

For the realization of those conditions, the pitching motions of the ship should be in resonance in nearly regular wave train. The wave model shown in Fig. 27, which satisfies those conditions, is suggested by an

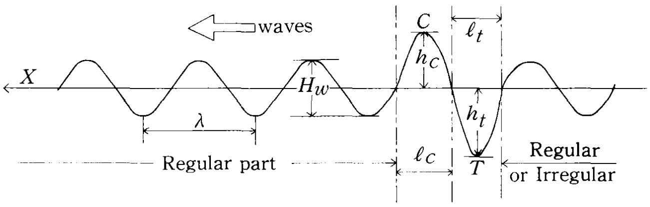

Fig.27 Modelled waves for serious bottom slamming

actual ship's disaster; the regular part of waves may induce the pitching motions, the bottom emerging in the crest C, and impacting on the trough T with high velocity. Due to dispersion, the waves take the model pattern only at a certain instant: they are expressed in the form of the superpositions of regular wave components by virtue of Fourier analysis, and its configurations in space are changed time to time.

The body plan of the bulk carrier used for the analysis

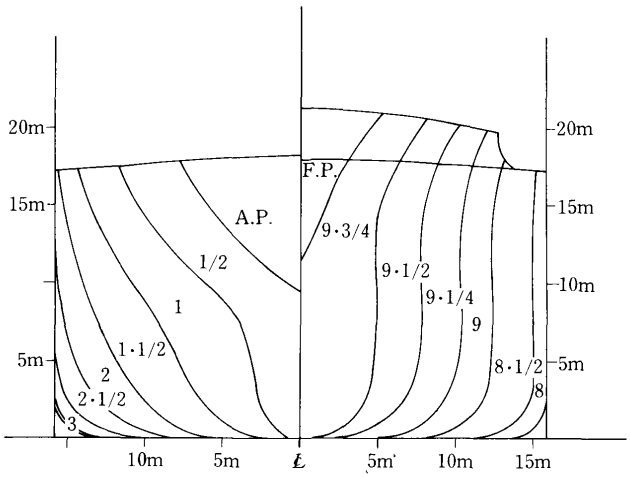

Fig.28 Body plan of bulk carrier

is shown in Fig. 28, which is characterized by the flat-bottom in the fore-body. The principal dimensions of the ship are as follows;

$$L \times B \times D = 216.4\,\mathrm{m} \times 31.7\,\mathrm{m} \times 17.3\,\mathrm{m}$$

$$d_{\mathrm{aft}} = 11.550\,\mathrm{m},\ d_{\mathrm{fore}} = 11.578\,\mathrm{m}$$

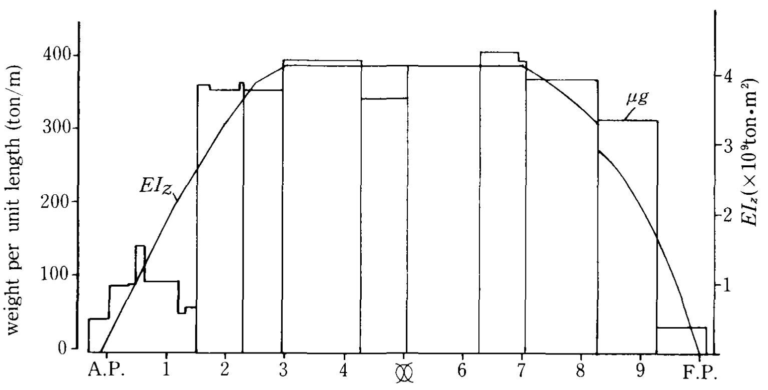

Fig.29 Weight and flexural rigidity distributions

The ship is in fully laden condition, and the weight and the flexural rigidity distributions are shown in Fig. 29. The logarithmic decrement of this ship is assumed as,[17]

$$\delta = 0.032$$

The surface elevation ζ and the velocity potential Φ of the incident waves are given by

$$\begin{cases} \zeta = \sum_{j=1}^{N} \zeta_i \cos(\varkappa_i X - \omega_i t + \varepsilon_i) \\ \Phi = -\sum_{i=1}^{N} (\omega_i/\varkappa_i)\,\zeta_i e^{-\varkappa_i z} \ \sin(\varkappa_i x - \omega_i t + \varepsilon_i) \end{cases} \tag{28}$$

were ζ_i, $\varkappa_i, \omega_i$, and ε_i are the amplitude, the wave number, the frequency, and the phase of the i-th component of the incident waves. According to the report with regard to the disaster of the ship,[15,16] the dimensions of the modelled wave for serious bottom slamming are chosen as,

$$\begin{cases} \lambda = 0.9L,\ l_c = \dfrac{0.9L}{2},\ l_t = \dfrac{0.8L}{2}, \\ H_w = 9\,\mathrm{m},\ h_c = 9\,\mathrm{m},\ h_t = 11\,\mathrm{m} \end{cases}$$

in Fig. 27.The wave length $\lambda_i\left(=\dfrac{2\pi}{\varkappa_i}=\dfrac{2\pi g}{\omega_i^2}\right)$,the amplitude ζ_i, and the phase ε_i of the wave components can be obtained by the FFT method as shown in Table 2.

Table 2 Wave components

i	λ_i/L	ζ_i(m)	ε_i(rad)
1	3.6	0.580	−2.075
2	1.8	0.992	2.475
3	1.2	0.874	−1.611
4	0.9	5.702	0.0
5	0.72	1.620	0.790
6	0.6	0.965	1.705
7	0.514	0.401	1.696
8	0.45	0.322	2.019
9	0.4	0.281	3.086
10	0.36	0.175	−3.080
11	0.327	0.177	2.031
12	0.3	0.141	1.934
13	0.277	0.057	−2.659

The sequence of the ship motions in the waves is shown in Fig.30. The high wave crest appears just before encountering with the ship, and the bottom emerges from the wave surface. In the course of bow-down, the trough becomes deeper, and the bottom plunges into the waves with the small inclination to the surface. The time history of the vertical bending moment at S.S. 8·1/2 is shown in Fig. 31, where t_s means the instant when the sagging bending moment comes to its maximum. The longitudinal distributions of bending moment and shearing force at t_s are shown in Fig.32. These results manifest the occurrence of the serious bottom slamming in full-bodied bulk carriers even in the fully laden condi-

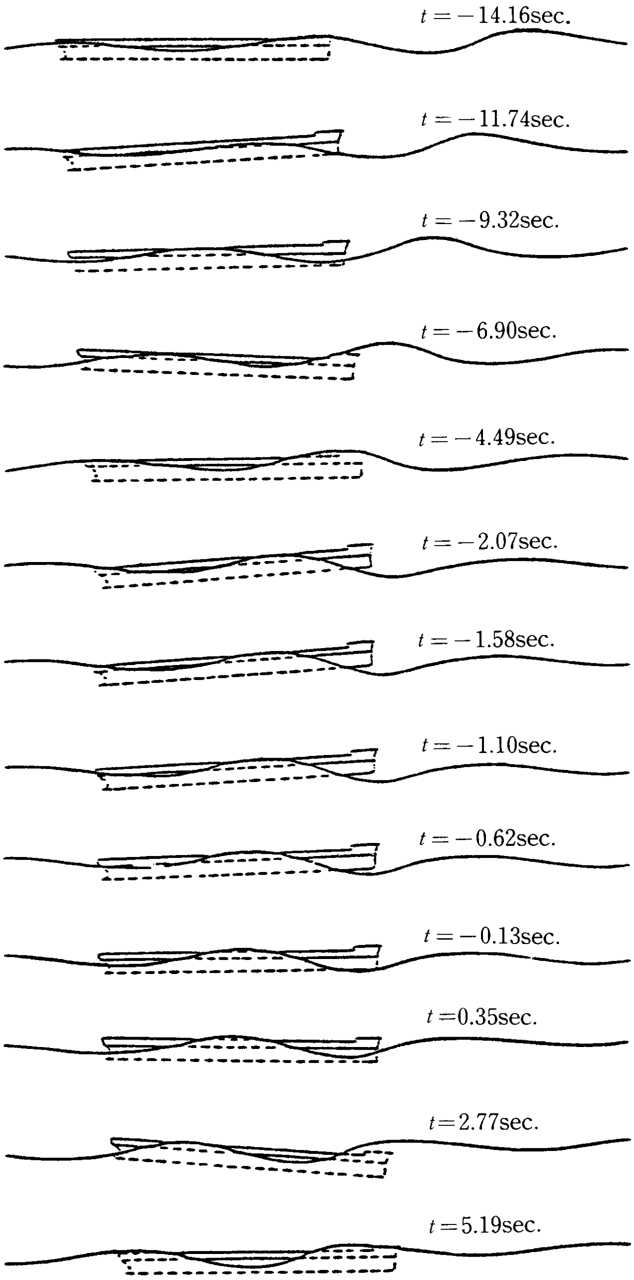

Fig.30 Ship motions in waves

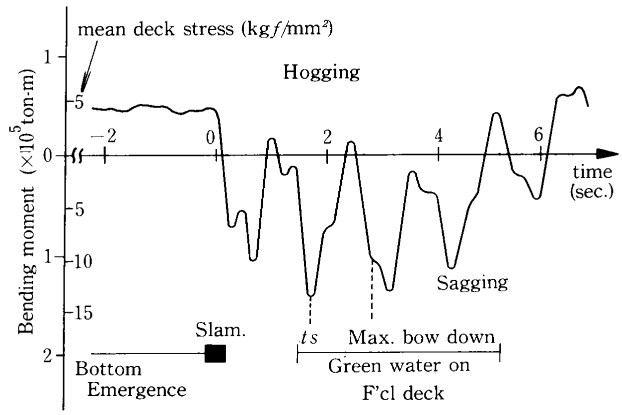

Fig.31 Time history of bending moment at S.S. 8·1/2

tions, due to an unhappy superposition of waves.

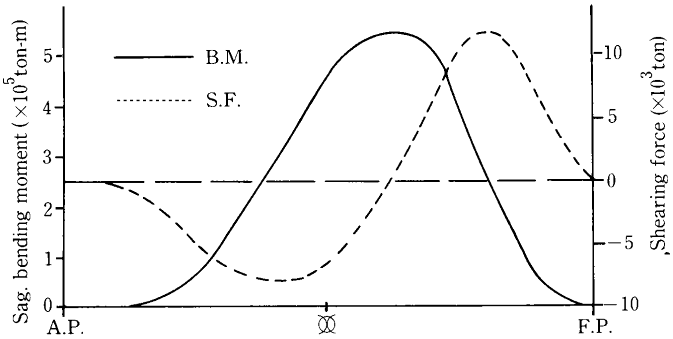

Fig.32 Longitudinal distributions of bending moment and shearing force at t_s

5. Discussions

The theory developed above gives satisfactory values for bending moments and shearing forces in general. As can be noticed, however, Eq.(1) is solved by the Galerkin method; Eq. (1) is satisfied in the sense of the weighted mean, and accordingly, it does not necessarily hold exactly in a certain region. This difficulty can be improved to some extent by minor change of the procedure.

The bending moment M is obtained by the formula

$$M_B=EI_z\left[\frac{\partial^2 w}{\partial x^2}+\eta\frac{\partial^3 w}{\partial t\partial x^2}\right] \cdots\cdots\cdots\cdots\cdots\cdots (29)$$

in the above standard procedure, which may have numerical errors because w is assumed to be a linear combination of only two terms. As an alternative method, bending moments can be obtained by integrating the sum of the external force and the inertia force two times along the ship's length; the results thus obtained are not in conformity to Eq. (1), but bending moments in the fore body will be improved to some extent.

In the present formulation, the wave bending moment is not derived directly, and this shortness can be improved by introducing the still water external force f_{es} and the corresponding displacement w_s;

$$\frac{\partial^2}{\partial x^2}\left[EI_z\frac{\partial^2 w_s}{\partial x^2}\right]=f_{es} \cdots\cdots\cdots\cdots\cdots\cdots\cdots (30)$$

Introduce the complementary displacement and external force, w_d and f_{ed} such that

$$\begin{cases} w_d=w-w_s \\ f_{ed}=f_e-f_{es} \end{cases} \cdots\cdots\cdots\cdots\cdots\cdots\cdots\cdots\cdots (31)$$

Then w_d satisfies Eq. (1) if f_e is replaced by f_{ed} which is derived from w and the wave configurations. The wave bending moment can be obtained by differentiating w_d or by integrating the sum of f_{ed} and the inertia force.

In reality, w_S is not definitely known for ordinary ships. Therefore, it is preferable to use an approximate method without using the displacement w_s corresponding to the still water bending moment. Let w_s^* be the solution of the following equation by the Galerkin procedure with the use of the same coordinate functions;

$$\frac{\partial^2}{\partial x^2}\left[EI_z\frac{\partial^2 w_s^*}{\partial x^2}\right]=f_{es} \cdots\cdots\cdots\cdots\cdots\cdots(32)$$

The corresponding bending moment is obtained by

$$M_{Bs}^*=EI_z\frac{\partial^2 w_s^*}{\partial x^2} \cdots\cdots\cdots\cdots\cdots\cdots(33)$$

Then the wave bending moment M_{Bw} is approximately given by

$$M_{Bw}\fallingdotseq M_B-M_{Bs}^*\equiv M_{Bw}^* \cdots\cdots\cdots\cdots\cdots\cdots(34)$$

and accordingly, the total bending moment is approximately given by

$$M_B\fallingdotseq M_{Bw}^*+M_{Bs} \cdots\cdots\cdots\cdots\cdots\cdots(35)$$

where M_{BS} is the still water bending moment obtained by the conventional method.

6. Conclusions

The longitudinal strength of ships in case of slamming were investigated taking account of nonlinearities. Calculations were performed for two typical ships; a fast container ship with large bow-flare in regular waves, and a full-bodied large bulk carrier in fully laden condition among irregular waves. As for the container ship, tank tests were carried out with the use of an elastic model to confirm the validity of the present theory. Conclusions obtained are as follows:

(1) The validity of the proposed nonlinear theory was confirmed by the experiments, and the theory is effective to clarify the responses of a ship due to slamming.

(2) As for a container ship, whipping is largely influenced by the interaction of bottom and bow-flare slamming. Serious slamming may occur for high speed, and the significant whipping vibrations are induced. Reduction of the ship's speed, however, decreases the whipping moments.

(3) In the case of full-bodied ships with deep fore draft, serious slamming may occur in swell-dominant seas even if the significant wave height is not extremely high.

References

1) P. Kaplan, T.P. Sargent, and A.I. Raff, "An Investigation of the Utility of Computer Simulation to Predict Ship Structural Response in Waves," SSC-197, 1969.

2) P. Kaplan, and T.P. Sargent, "Further Studies of Computer Simulation of Slamming and Other Wave-Induced Vibratory Structural Loadings on Ships in Waves," SSC-231, 1972.

3) R.E.D. Bishop, W.G. Price, and P.K.Y. Tam, "A Unified Dynamic Analysis of Ship Response to Waves," Trans. RINA,Vol.119,1977.

4) R.E.D. Bishop, W.G. Price, and P.K.Y. Tam, "On the Dynamics of Slamming," Trans. RINA, Vol. 120,1978.

5) R.E.D. Bishop, and W.G. Price, Hydroelasticity of Ships, Cambridge University Press, 1979.

6) W.K. Meyerhoff, and G. Schlachter, "Ein Ansatz zur Bestimmung der Belastung von Schiffen im Seegang unter Berücksichtigung Hydrodynamischer Stösse," JSTG, Bd.71, 1977.

7) Y. Yamamoto, M. Fujino, and T. Fukasawa, "Motion and Longitudinal Strength of a Ship in Head Sea and the Effects of Non-Linearities," JSNA, Japan, Vols. 143 and 144, 1978, Vol. 145, 1979 (in Japanese); Naval Architecture and Ocean Engineering, Vol.18, Soc. Naval Arch. Japan, 1980.

8) Y. Yamamoto, M. Fujino, T. Fukasawa, and H. Ohtsubo, "Slamming and Whipping of Ships Among Rough Seas," Numerical Analysis of the Dynamics of Ship Structures, EUROMECH 122, ATMA, 1979.

9) E.V. Lewis, "Ship Model Tests to Determine Bending Moments in Waves," Trans. SNAME, Vol. 62, 1954.

10) R. Wereldsma, and G. Moeyes, "Wave and Structural Load Experiments for Elastic Ships," Proc. 11th Symposium on Naval Hydrodynamics, 1976.

11) T.Fukasawa, Y. Yamamoto, M. Fujino, and S. Motora, "Motion and Longitudinal Strength of a Ship in Head Sea and the Effects of Non-Linearities (4th Report)-Experiments, "JSNA, Japan, Vol. 150, 1981; Naval Architecture and Ocean Engineering, Vol. 20, Soc. Naval Arch. Japan, 1982.

12) T. Kumai, "Damping Factors in the Higher Modes of Ship Vibration," European Shipbuilding, Vol.7, 1958.

13) Y.Kumakura, T. Nagano, Y. Okumoto, and K. Tanida, "Measurements on the Strength of Container Ship in Service," JSNA, Japan, Vol.136, 1974 (in Japanese).

14) R. Wereldsma, "Fundamentals of Experiments on Models of Elastic Seaborne Structures, A Tankery Problem," Ship Structures Laboratory, Delft Univ. of Technology, Rep. No.187,1974.
15) Y. Yamamoto, M. Fujino, H. Ohtsubo, T. Fukasawa, G. Aoki, H. Ikeda, and A. Kumano, "Analysis of Disastrous Structural Damage of a Bulk Carrier," Proc. 2nd Int. Symp. on Practical Design in Shipbuilding, PRADS 83, 1983. (to be published).
16) Y. Yamamoto, M. Fujino, H. Ohtsubo, T. Fukasawa, Y. Iwai, G. Aoki, I. Watanabe, H. Ikeda, A. kumano, and T. Kuroiwa, "Disastrous Damage of a Bulk Carrier due to Slamming," JSNA, Japan, Vol. 154, 1983. (in Japanese) (to be published).
17) G. Aertssen, and R. De Lambre, "A Survey of Vibration Damping Factors found from Slamming Experiments on Four Ships," Trans. NECIES, Vol. 87, 1970-71.